

Microaneurysm Detection in Fundus Images

Mr. Abhinandan Kalita, Assistant Professor,

Department of Electronics & Communication Engineering, GMT-Guwahati, Assam, India.

abhinandan_ece@gimt-guwahati.ac.in; abhinandan.kalita@gmail.com

Abstract— Diabetic patients suffer from diabetic retinopathy due to prolonged diabetes. Microaneurysms are the first clinical abnormality found in the eye of a diabetic patient. This paper deals with some image processing operations to extract microaneurysms with the help of a few innovative texture features for the analysis of diabetic retinopathy. The performance of the proposed method stands out prominent in terms of specificity and accuracy. It gives an average specificity of 93.7% and average accuracy of 97.6%. The algorithm is tested using images taken from DRIVE database.

Keywords- diabetic retinopathy, blood vessels, microaneurysm, fundus image

I. INTRODUCTION

The first signs of diabetic retinopathy are called microaneurysms. They are small circular shaped bulges developed from the weak blood vessels and are the earliest clinical sign of diabetic retinopathy. The number of microaneurysms increases with the stage of the retinopathy and therefore, it is extremely important to detect them during the early stages of development. They appear in clusters as tiny dark red spots (hemorrhages) in the retina. Their sizes range from 10-100 microns. Microaneurysm detection in the early stage can reduce the degree of blindness. The other significant symptoms of diabetic retinopathy are appearance of exudates and abnormal growth of blood vessels. Diabetic retinopathy has four different stages [1] namely mild non-proliferative, moderate non-proliferative, severe non-proliferative and proliferative diabetic retinopathy.

In this paper, we have proposed a feature extraction method with the help of a few innovative texture based features for an automatic diabetes recognition system. We have extracted the microaneurysms which can later be fed to an artificial neural network environment for classification purpose.

Chapter II contains the material being used. Chapter III gives the tabulated list of literature survey. Chapter IV describes the design and implementation of the proposed algorithm. Chapter V gives the result and comparison of our algorithm. Chapter VI contains the conclusion and future work.

II. MATERIAL

Retinal images are taken with the help of a fundus camera. In the initial algorithm development stage, we have used images captured by a fundus camera with a 45 degree field of view taken at Omega Eye Clinic and Research Centre, Guwahati, India. The images were stored in TIFF (.tif) file format. For the validation purpose, we have used images from DRIVE database.

III. LITERATURE SURVEY

Some of the related works are listed in Table I.

IV. DESIGN AND IMPLEMENTATION OF THE PROPOSED TECHNIQUES

Here, we have proposed a feature extraction method for the extraction of microaneurysms. The overall block diagram of feature extraction is shown in figure 1.

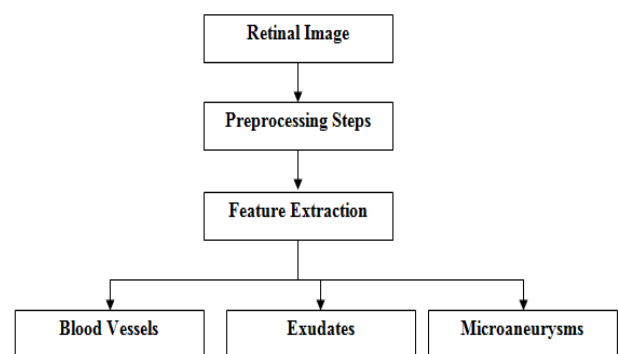


Figure1. Block diagram of feature extraction

A. Morphological Image Processing

If $f(u, v)$ is a finite size grayscale image defined in

Z^2 and B is a binary structuring element then

Dilation:

$$(f \oplus B)(u, v) = \max\{f(u-s, v-t) \mid (s, t) \in B\}$$

Erosion:

$$(f \square B)(u, v) = \min\{f(u+s, v+t) \mid (s, t) \in B\}$$

$$\text{Opening: } f \circ B = (f \square B) \oplus B$$

$$\text{Closing: } f \bullet B = (f \oplus B) \square B$$

TABLE I. SOME RELATED WORKS

SL. No.	AUTHORS/YEAR	TECHNIQUES	DATABASE	COLOUR SPACE	SENSITIVITY (%)	SPECIFICITY (%)	ACCURACY (%)
1	KRISHNA ET AL. [2] (2013)	Ensemble-based microaneurysms detector, Walter Klein, and CLACHE	MESSIDOR	GRAY SCALE	-	-	-
2	ROY ET AL. [3] (2013)	Canny edge detection, morphological reconstruction	DIARETD B1	GREEN CHANNEL	89.5	82.1	-
3	ADAL ET AL. [4] (2013)	Contrast enhancement technique, Hessian-based candidate selection algorithm, and SVM classifier	ROC	GREEN CHANNEL	-	44.64	-
4	DING AND MA [5] (2014)	Dynamic multiparameter template (DMPT) matching scheme	ROC	-	96	-	-

B. Texture Properties:

Texture analysis shown in figure 2 gives the description of an image in terms of variations in the pixel intensities or gray level.

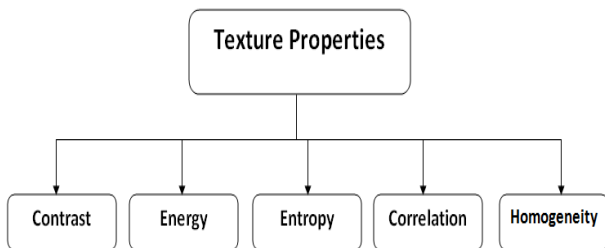


Figure2. Texture Analysis

Gray-Level Co-occurrence Matrix (GLCM) is the computation of the frequency of each pixel pair occurring for different combinations of pixel brightness values in an image. The function “graycomatrix” is used to create the GLCM of the grayscale image. It calculates how often the pixel with value i of the gray level occurs horizontally adjacent to another pixel with value j. Each element (i,j) in the GLCM represents frequent of occurrence. The function “graycoprops” normalizes the GLCM so that the sum of its elements is equal to 1. It calculates the statistics as specified in the property.

Homogeneity is the measurement of the closeness of the distribution of elements in the GLCM to the GLCM diagonal and returns a value between 0 and 1. The homogeneity formula is as follows:

$$\sum_{i,j} \frac{p(i,j)}{1+|i-j|}$$

Contrast: Returns a measure of the intensity contrast between a pixel and its neighbour over the whole image. Range = [0 (size (GLCM, 1)-1) ^2]. The formula for contrast is as follows:

$$\sum_{i,j} |i-j|^2 p(i,j)$$

Correlation: Returns a measure of how correlated a pixel is to its neighbour over the whole image. Range = [-1 1]. Correlation is 1 or -1 for a perfectly positively or negatively correlated image. The formula for correlation is as follows:

$$\sum_{i,j} \frac{(i-\mu_i)(j-\mu_j)p(i,j)}{\sigma_i\sigma_j}$$

Energy: Returns the sum of squared elements in the GLCM. Range = [0 1]. The formula for energy is as follows:

$$\sum_{i,j} p(i,j)^2$$

Entropy is the statistical measure of the randomness of the grayscale image’s texture. The green component of the image is applied with adaptive histogram equalization twice to enhance its contrast and texture. The function “entropy” is then used on the image which returns a scalar value. This represents the entropy of intensity for the image.

C. Extraction of Microaneurysms:

Figure 3 shows the block diagram of the proposed microaneurysm extraction technique. The grayscale image is used to detect the circular border and optical disc mask. The green channel of the image first finds the edges using canny method before removing the circular border to fill the enclosed small area. The larger areas are then removed and applied with AND logic to remove the exudates. The blood vessels and optical disc are then removed to obtain the microaneurysms.

V. EXPERIMENTAL RESULTS AND COMPARISONS

The performance of the proposed algorithm is tested using MATLAB version 7.11.0 (R 2010b) with the help of a publicly available DRIVE database. The performance of the proposed microaneurysm extraction results are analyzed with respect to the ground truth images. We have also extracted microaneurysms of the images taken from Omega Eye Clinic and Research Centre, Guwahati, India but could not evaluate the performance of those images due to the absence of ground truth images. Table II summarize the results of this proposed work using DRIVE database. The proposed

algorithm detects and segments the microaneurysms at an average specificity of 93.7% and accuracy of 97.6% respectively. The results obtained are compared with the other state of art and tabulated in Table III. Table IV shows the texture properties of the DRIVE database images. Table V shows the texture properties of images taken from Omega Eye Clinic and Research Centre, Guwahati, India

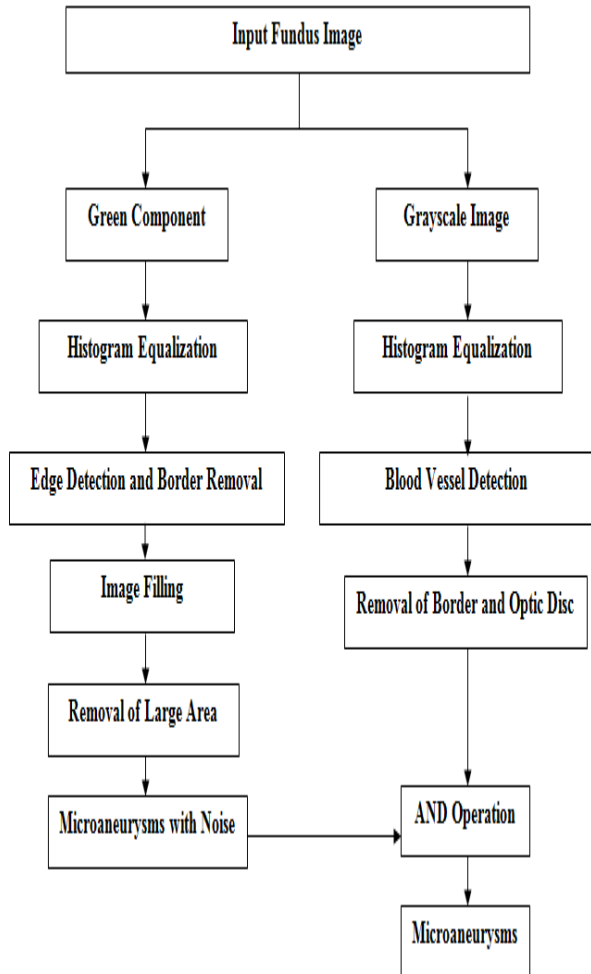


Figure3. Block diagram of microaneurysm extraction

TABLE II. TABLE SHOWING AVERAGE SPECIFICITY AND ACCURACY USING DRIVE DATABASE

Database	Average Specificity	Average Accuracy
DRIVE	93.7%	97.6%

TABLE III. MICROANEURYSM EXTRACTION RESULTS (DRIVE DATABASE)

Method	Year	Specificity (%)	Accuracy (%)
ROY ET AL. [3]	2013	82.1	-
ADAL ET AL. [4]	2013	44.64	-
DATTA ET AL. [6]	2013	82.64	99.98
PROPOSED METHOD	2018	93.7	97.6

TABLE IV. TEXTURE PROPERTIES (DRIVE DATABASE)

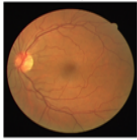
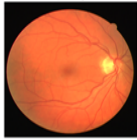
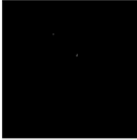

Feature	DRIVE Database: Test Image 1	DRIVE Database: Test Image 2
Fundus Image		
Microaneurysms	 Area=27	 Area=58
Correlation	0.9876	0.9913
Energy	0.3469	0.3498
Entropy	7.831	7.8540
Homogeneity	0.9777	0.9798
Contrast	0.0522	0.0441

TABLE V. TEXTURE PROPERTIES (IMAGES TAKEN FROM OMEGA EYE CLINIC AND RESEARCH CENTRE, GUWAHATI, INDIA)

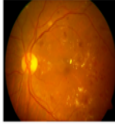
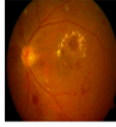


Feature	Sankardev Netralaya Eye Hospital, Guwahati: Test Image 1	Sankardev Netralaya Eye Hospital, Guwahati: Test Image 2
Fundus Image		
Microaneurysms	 Area=482	 Area=738
Correlation	0.9796	0.9699
Energy	0.2222	0.2611
Entropy	7.6868	7.6655
Homogeneity	0.9721	0.9727
Contrast	0.0579	0.0568

Figure 4 shows a set of images taken from Omega Eye Clinic and Research Centre, Guwahati, India where a) the first image is the original input fundus image, b) the second one is the green component image, c) the third is the grayscale image, d) the fourth image is the image and histogram after first adaptive histogram equalization, e) the fifth image is the image and histogram after second adaptive histogram equalization, f) the sixth image is the edges of image for circular border detection, g) the seventh image is the result of image fill, dilation and erosion h) the eighth image is the new circular border image, i) the ninth image is the image with blood vessels and noise, j) the tenth image is the area of microaneurysm after removing blood vessels and noise k) the eleventh image is the final microaneurysm image.



Figure4 (a) Input Fundus Image

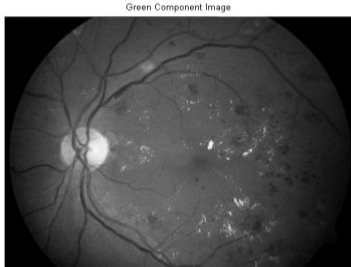


Figure4 (b) Green Component Image

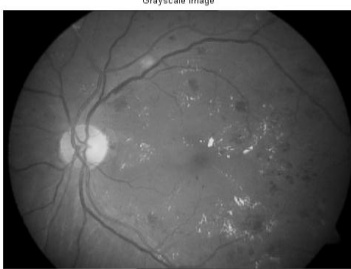


Figure4 (c) Grayscale Image

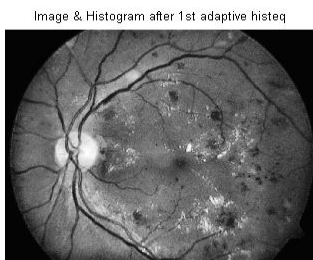


Figure4 (d) Image and Histogram (1st adaptive histeq)

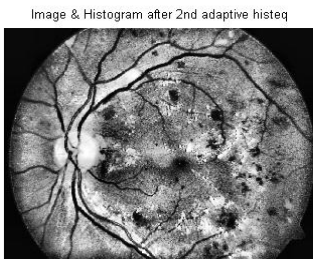


Figure4 (e) Image and Histogram (2nd adaptive histeq)

Fig. 6. Edges of image for Cborder Detection

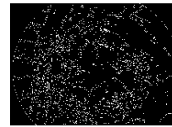


Figure4 (f) Edges of Image for Circular Border Detection

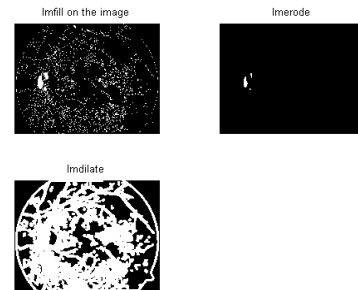


Figure4 (g) Image Fill, Dilation, Erosion

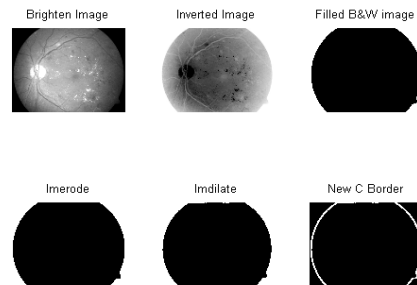


Figure4 (h) New Circular Border

Blood vessels and noise after im2bw

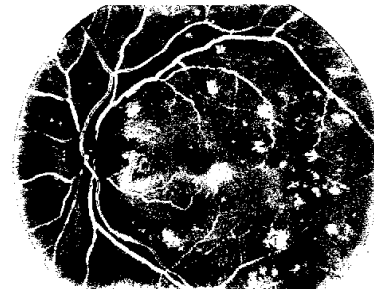


Figure4 (i) Blood Vessels and Noise

Area of microaneurysms after removing blood vessels & noise

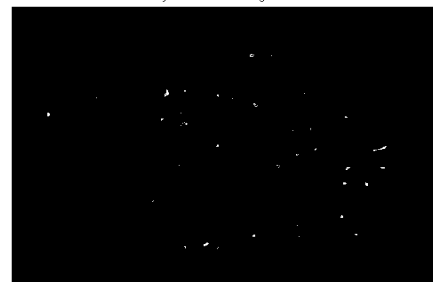


Figure4 (j) Area of Microaneurysm after Removing Blood Vessels and Noise

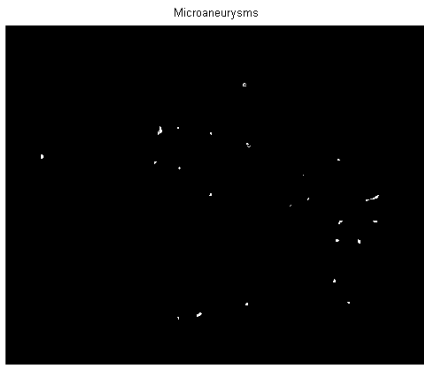


Figure4 (k) Microaneurysms

VI. CONCLUSION

From the experimental results shown in tables II, III, IV and V, it can be concluded that the proposed method leads to a satisfactory result in terms of specificity and accuracy. It gives an average specificity of 93.7% and average accuracy of 97.6%. This work can be further extended to extract exudates and abnormal growth of blood vessels from the retinal images. The extracted features can be fed to an artificial neural network environment for further processing.

REFERENCES

- [1] N. Amrutkar, Y. Bandgar, S. Chitalkar, S.L. Tade, "Retinal blood vessel segmentation algorithm for diabetic retinopathy and abnormality detection using image subtraction," International Journal of Advanced Research in Electrical, Electronics and Instrumentation Engineering, Vol.2, Issue 4, April 2012.
- [2] N. Venkata Krishna, N. Venkata Siva Reddy, M. Venkata Ramana, E. Prasanna Kumar, "The Communal System for Early Detection Microaneurysm and Diabetic Retinopathy Grading Through Color Fundus Images," International Journal of Scientific Engineering and Technology, Volume 2 Issue 4, pp : 228-232, ISSN : 2277-1581, 1 April 2013.
- [3] Rukhmini Roy, Srinivasan Aruchamy, Partha Bhattacharjee, "Detection of Retinal Microaneurysms using Fractal Analysis and Feature Extraction Technique," International conference on Communication and Signal Processing, April 3-5, 2013, India.
- [4] Kedir Adal, Sharib Ali, Desire Sidibe, T.P. Karnowski, Edward Chaum, Fabrice Meriaudeau, "Automated detection of microaneurysms using robust blob descriptors," SPIE Medical Imaging - Computer-Aided Diagnosis, Orlando - FL, United States. pp.8670-22, Feb 2013.
- [5] Shan Ding and Wenyi Ma, "An Accurate Approach for Microaneurysm Detection in Digital Fundus Images," IEEE 22nd International Conference on Pattern Recognition, pp. 1846-1851, 2014.
- [6] Niladri Sekhar Datta, Himadri Sekhar Dutta, Mallika De, Saurajeet Mondal, "An Effective Approach: Image Quality Enhancement for Microaneurysms Detection of Non Dilated Retinal Fundus Image," Elsevier: International Conference on Computational Intelligence: Modeling Techniques and Applications, Procedia Technology, pp. 731 - 737, 2013.
- [7] G. B. Kande, P. V. Subbaiah, T. S. Savithri, "Feature extraction in digital fundus images," Journal of Medical and Biological Engineering, vol. 29, No. 3, 2009.
- [8] M.Goldbaum, S.Moezzi, A. Taylor, S. Chatterjee, J. Boyd, E. Hunter, and R.Jain, "Automated diagnosis and image understanding with object extraction, object classification and

- interferencing in retinal images," International Conference on Image Processing, vol. 3, p.695698, September 1996.
- [9] A.Osareh, B.Shadgar, and R.Markham, "A computational-intelligence-based approach for detection of exudates in diabetic retinopathy images," IEEE Transaction on Information Technology in Biomedicine, vol.13,p.535545, July 2009.
- [10] Y.Hatanaka, T.Nakagawa, Y.Hayashi, T.Hara, and H.Fujita, "Improvement of automated detection method of hemorrhages in fundus images," in 30th Annual International IEEE EMBS Conference, August 2008.
- [11] A. Youssif, A. Ghalwash, and A. Ghoneim, "Optic disc detection from normalized digital fundus images by means of a vessels direction matched filter," IEEE Transactions on Medical Imaging, vol.27,p.1118, January 2008.
- [12] M. Neimeijer, B. Ginneken, M. Cree, A. Mizutani, G. Quellec, C. Sanchez, B. Zhang, R. Hornero, M. Lamard, C.Muramatsu, X.Wu, G. Cazuguel, J.You, A.Mayo, Q.Li, Y. Hatanaka, B.Coeheuer, C.Roux, F. Karray, M.Garca, H. Fujita, and M. Abramo, "Retinopathy online challenge Automatic detection of microaneurysms in digital color fundus photographs," IEEE Transactions on Medical Imaging, vol.29,pp. 185- 195, January 2010.
- [13] L. Zhang, Q. Li, J. You, and D. Zhang, "A modified matched filter with double sided thresholding for screening proliferative diabetic retinopathy," IEEE Transactions on Information Technology in Biometrics, vol.13,pp. 528-534, July 2009.
- [14] T. Walter, P. Massin, A. Erginay, R. Ordonez, C. Jeulin, and J.C. Klein, "Automatic detection of microaneurysms in color fundus images," Medical Image Analysis, vol. 11,pp.555-566, May 2007.
- [15] G. Quellec, M. Lamard, P. Josselin, G. Cazuguel, and C. Roux, "Optimal wavelet transform for the detection of microaneurysms in retinal photographs," IEEE Transactions on Medical Imaging, vol.27, p. 12301241, Sept.2008.
- [16] Junichiro Hayashi, Takamitsu, Joshua Cole, Ryusuke Soga, Yuji Hatanaka, Miao Lu, Takeshi Hara, and Hiroshi Fujita, "A development of computer-aided diagnosis system using fundus images," Proceeding of the 7th International Conference on Virtual Systems and Multimedia(VSMM 2001), pp.429-438,sept2001.
- [17] N.Singh and R.C.Tripathi, "Automated early detection of diabetic retinopathy using image analysis techniques," International Journal of computer Applications, vol.8, No.2, pp.18-23, Oct.2010.
- [18] Vallabha,D.,Dorairaj,R., Namuduri K.R., and Thompson, H., "Automated detection and classification of vascular abnormalities in diabetic retinopathy," 38th Asilomar Conference on Signals, Systems and Computers, Nov2004.
- [19] Y.F. Ming, "Identification of diabetic retinopathy stages using digital fundus images using imaging," Master's thesis, School of Science and Technology, SIM University, 2009.
- [20] Akara Sopharak, Bunyarit Uyyanonvara, Sarah Barman and Tom Williamson, "Automatic Microaneurysm Detection from Non-dilated Diabetic Retinopathy Retinal Images," Proceedings of the World Congress on Engineering, Vol II, WCE 2011, London, U.K, July 2011.
- [21] Luca Giancardo, Fabrice Meriaudeau, Thomas P. Karnowski, Kenneth W. Tobin, Yaqin Lic and Edward Chaum, M.D., "Microaneurysms Detection with the Radon Cliff Operator in Retinal Fundus Images," Proceedings. of SPIE, Vol. 7623, 2010.